CSIRO PUBLISHING

International Journal of Wildland Fire **2010**, *19*, 698–704 www.publish.csiro.au/journals/ijwf

Field estimation of ash and char colour-lightness using a standard grey scale

David P. Roy[A,E], *Luigi Boschetti*[B], *Stefan W. Maier*[C] *and Alistair M. S. Smith*[D]

[A]Geographic Information Science Center of Excellence, South Dakota State University, Brookings, SD 57007, USA.
[B]Department of Geography, University of Maryland, College Park, MD 20740, USA.
[C]School of Environmental and Life Sciences, Charles Darwin University, Darwin, NT 0909, Australia.
[D]Department of Forest Resources, University of Idaho, ID 83844, USA.
[E]Corresponding author. Email: david.roy@sdstate.edu

Abstract. Vegetation fires produce biomass combustion residues, with colour varying from dark black char to white mineral ash. The colour-lightness of char and ash combustion residues is a qualitative parameter describing the post-fire condition of burned areas, and has been correlated with the completeness of combustion, fire intensity, and fire duration. Researchers have suggested that visual comparison of combustion residue samples with a standard grey scale would enable reliable combustion residue colour-lightness estimation. This paper describes an experiment aimed at assessing if colour-lightness can be estimated using a standard grey scale. Fifteen combustion residue samples with colour-lightness ranging from black char to white mineral ash were collected in the Northern Territory, Australia, and visually evaluated by three individuals using a grey scale. The grey-scale scores (0–19) were compared with the mean visible (390 to 830 nm) wavelength combustion residue reflectance (0–1) measured with a portable spectroradiometer. A significant linear relationship between the grey-scale scores and the mean visible combustion residue reflectance was found ($R^2 = 0.816$ with a linear fit, $R^2 = 0.936$ with a logarithmic-transformed fit). This finding suggests that combustion residue colour-lightness can be assessed in the field using inexpensive grey scales, and that this technique is a suitable avenue for future research on the field assessment of fire characteristics and effects.

Introduction

Vegetation fires produce biomass combustion residues, with colour varying from dark black char, the primary by-product following pyrolysis of volatiles in vegetation, to white mineral ash, produced when vegetation has undergone complete or near-complete combustion. White ash can be deposited by energetic grass fires that last for seconds and can also be produced within fires burning large fuel items (e.g. logs and tree branches) over periods of days (Smith and Hudak 2005). Although it is possible to attain a spatially continuous coverage of black char across a landscape, white ash is generally spatially discontinuous and patchy. Combustion residues have different shades of grey owing to the mixing of black char and white ash in different proportions (Smith *et al.* 2005).

Studies have demonstrated that the abundance of black char and white ash is a correlate of various post-fire effects and that the colour-lightness of combustion residues is related to the fire intensity, combustion completeness, and fire duration (Stronach and McNaughton 1989; McNaughton *et al.* 1998; Landmann 2003; Roy and Landmann 2005; Smith *et al.* 2005, 2007; Lentile *et al.* 2009). The fire intensity refers to the rate of energy release, usually the energy released per length of fire front ($W\,m^{-1}$) (Byram 1959). The combustion completeness (unitless) is the fraction of fuel exposed to the fire that actually burns (Scholes *et al.* 1996; Shea *et al.* 1996). These variables are important for understanding the effects of fire on vegetation structure and ecosystem processes (Trollope and Tainton 1986; Williams *et al.* 1998) and for estimating the amount of biomass burned and therefore trace gas and particulate emissions to the atmosphere (Wooster *et al.* 2005). McNaughton *et al.* (1998) suggested that relationships between the colour-lightness of combustion residues and ground measurements of fire characteristics could be used to calibrate remote-sensing methods capable of retrospectively estimating fire characteristics over large areas.

Satellite data have been used to monitor fire for more than two decades using computer algorithms that detect the location of active fires at the time of satellite overpass, and in the last decade using burned area mapping algorithms that map the spatial extent of the areas affected by fires (Lentile *et al.* 2006; Roy *et al.* 2008). Char and ash reflectance cannot be retrieved reliably on a systematic basis from satellite sensor data, however, because of factors including the spatial heterogeneity of the fuel load, fire behaviour and area burned, relative to the satellite sensor spatial resolution. Smith *et al.* (2005) observed a quadratic relationship between the change in reflectance due to vegetation fire and the fire duration, effectively charting the decrease in reflectance from vegetation to black char and subsequent increase in reflectance to white mineral ash. Roy and Landmann (2005) demonstrated, using a simple spectral

© IAWF 2010 10.1071/WF09133 1049-8001/10/060698

mixture model of fire effects, and by comparing ground measurements with 30-m Landsat satellite data, that the change in reflectance due to vegetation fire was linearly related to the combustion completeness multiplied by the areal proportion of the pixel affected by fire. Smith *et al.* (2005) and Smith and Hudak (2005) noted that sensors with spatial resolutions higher than those of 30-m Landsat sensors are generally required if patches of white ash are to be used to infer fire characteristics. In addition to spatial resolution issues, the persistence of char and ash depends on rates of dissipation by wind and rain, and so remotely sensed char and ash reflectance can change rapidly relative to daily polar-orbiting satellite observation frequencies (Trigg and Flasse 2000). These satellite remote-sensing spatial and temporal resolution constraints may be reduced if airborne platforms are used. However, with all airborne and satellite remotely sensed data, the burned surface can be obscured by overstorey tree canopy and vegetation cover (Pereira *et al.* 2004) and it may be difficult to differentiate between char and ash and other scene elements, for example, between white ash and highly reflective soil, or between black char and dark soils or shadows (Souza *et al.* 2005). Ground-based measurement of reflectance with portable field spectroradiometers largely overcomes these issues (Trigg and Flasse 2000; Landmann 2003; Smith *et al.* 2005) but field spectroradiometers require specialised expertise to operate and are expensive and delicate instruments that cannot be used to quickly measure reflectance over large areas.

Stronach and McNaughton (1989) noted significant relationships between relative visual rankings of combustion residue colour-lightness and fire properties, and suggested that visual comparison of combustion residue samples with a standard grey scale would enable more reliable colour-lightness estimation. Grey scales are available as printed sheets with graduations of grey from black to white and are used to calibrate photographic equipment (Eismann and Duggan 2008). They are very inexpensive and simple to use compared with field spectroradiometers, and so provide the potential for rapid assessment of combustion residue colour-lightness over large areas. The purpose of this paper is to establish if combustion residue colour-lightness can be estimated using a standard grey scale. This is achieved by comparison of grey-scale colour-lightness assessments with visible wavelength spectroradiometer reflectance measurements of char and ash samples selected to encompass a range of colour-lightness.

Study site

Field measurements were made in the early dry season (July 2009) around the Western Arnhem Land Fire Abatement (WALFA) project Kabulwarnamyo field base camp, located ~300 km east of Darwin, Northern Territory, Australia. The WALFA study site is on the Arnhem Plateau, a tropical savanna monsoonal system with a very low population density (<0.01 persons km^{-2}) and covering ~24 000 km^2 (Edwards and Russell-Smith 2009). The landscape comprises sandstone heaths and low open woodlands, comprising many obligate seeder shrub species with scattered emergent trees interspersed with highly flammable hummock spinifex grasses and with open conifer and evergreen rainforest communities, primarily *Callitris intratropica* and *Allosyncarpia ternate* (Yates *et al.* 2008; Edwards and Russell-Smith 2009). Approximately 35% of the landscape was fire-affected on average annually for the period 1997–2005, with most fires occurring in the late dry season under severe fire-weather conditions (Yates *et al.* 2008).

Method

Combustion residue collection

Several prescribed fires were lit in conjunction with prefire, burning, and post-fire ground and helicopter measurements in support of the WALFA project (Russell-Smith *et al.* 2009). Ash and char samples were collected opportunistically over a 3-day period immediately after fires had burned and up to 1 day post fire. Samples were collected from burned grasses, tree limbs, and trunks. A total of 15 samples were selected to encompass as much as possible the complete range of combustion residue colour-lightness from black to white. This was challenging and only homogeneous patches with uniform combustion residue colour and covering an area of at least 10 × 10 cm were selected; this area was selected through trial and error as providing sufficient residue material for subsequent measurement. A digital photograph was taken to document the sample (Fig. 1). The combustion residues were then collected carefully, by picking or brushing them into a plastic collection bag. Wind-blown and fallen twigs, leaves, soil, termite fecal matter, and any other non-burned material were not collected. Only the top ~3–5 mm of the combustion residues were collected.

Combustion residue colour-lightness assessment

Measurement conditions

Within 2 hours of collection, the combustion residues in each sample were mixed thoroughly and placed on a table in a small ~5 × 5-cm flattened heap. The table was located outside, surrounded by a wind shield oriented not to shadow the sample. The measurements were made under windless conditions, but even so, the combustion residue samples containing finer white ash samples were susceptible to air disturbances. All measurements were made under normal direct and diffuse midday sun with minimal cloud cover.

Grey-scale measurement

A Tiffen Q-13 (B&H photo, New York) grey scale consisting of a 20 × 4-cm cardboard strip with 20 calibrated grey scales from white (score 0) to black (score 19) was used (shown in Fig. 1). The combustion residue sample colour-lightness was independently estimated by three individuals by placing the grey scale adjacent to the flattened combustion residue heap and making a subjective visual assessment of the grey-scale value (0–19) that most closely matched the combustion residue colour-lightness. Care was taken to ensure that the samples were measured in random order and that the three individuals did not communicate their scores; this was in an attempt to ensure that any systematic differences between their assessments were maintained over all 15 samples.

Reflectance spectra measurement

The reflectance spectrum of each combustion residue sample was measured using an ASD Field Spec Pro portable

Fig. 1. Example of an *in situ* combustion residue sample and the corresponding grey scale (top).

field spectroradiometer (ASD Inc., Boulder, CO). The spectrometer fibre-optic cable was placed 5 cm vertically above the centre of the flattened combustion residue heap, yielding an approximately 2.2 cm-diameter circular sensing area. A total of 300 spectra were recorded for each sample, and then the mean spectra derived. The reflectance (0–1) was output every nanometer, although the spectrometer visible wavelength spectral resolution was 3 nm (Analytical Spectral Devices 2002). Before each combustion residue sample was measured, the reflectance of a Spectralon reflectance panel (Labsphere Inc., North Sutton, NH) was measured. The Spectralon reflectance panel can be considered an ideal reflectance standard because of its almost perfectly Lambertian reflectance characteristics and high durability in field conditions (Sanches *et al.* 2009). After the field measurements were taken, the Spectralon panel was calibrated in a laboratory using a National Institute of Standards and Technology traceable Spectralon calibration target and the resulting calibration information used to calibrate the combustion residue reflectance spectra using standard approaches.

Conversion of reflectance spectra to mean visible reflectance

For each of the 15 combustion residue spectra, a single mean weighted visible reflectance value taking into account the spectral response of a typical human eye under natural daylight conditions was computed as:

$$\bar{\rho}_{eye} = \sum_{\lambda=390}^{830} V(\lambda)\,\rho_\lambda \Big/ \sum_{\lambda=390}^{830} V(\lambda) \qquad (1)$$

where $\bar{\rho}_{eye}$ is the mean weighted visible reflectance taking into account the spectral response of a typical human eye, $V(\lambda)$ is the typical human eye spectral response function (0–1) for natural daylight conditions, and ρ_λ is the spectroradiometer-measured reflectance (0–1) at wavelength λ. The spectral response $V(\lambda)$ function was defined by a recently published luminous efficiency function for daylight adaptation that improves on the original International Lighting Commission definition (Sharpe *et al.* 2005). Fig. 2 shows the luminous efficiency function, illustrating daylight human vision from 390 to 830 nm and how the response is highly spectrally dependent.

In addition, the mean visible wavelength (390 to 830 nm) reflectance value was computed as:

$$\bar{\rho} = \sum_{\lambda=390}^{830} \rho_\lambda \Big/ 441 \qquad (2)$$

where $\bar{\rho}$ is the mean visible reflectance and ρ_λ is the spectroradiometer-measured reflectance (0–1) at wavelength λ.

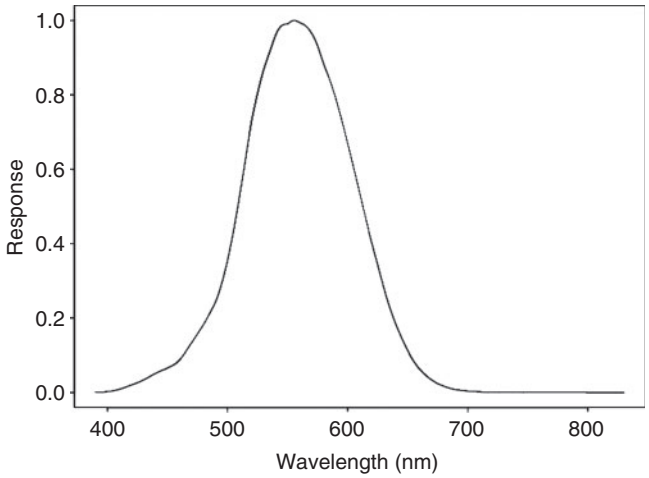

Fig. 2. Luminous efficiency function for daylight adaptation, i.e. the spectral response of a typical human eye (Sharpe *et al.* 2005). These data are available at http://journalofvision.org/5/11/3/extra/index.html (accessed 30 March 2010) and are non-negligible for the plotted wavelengths 390 to 830 nm.

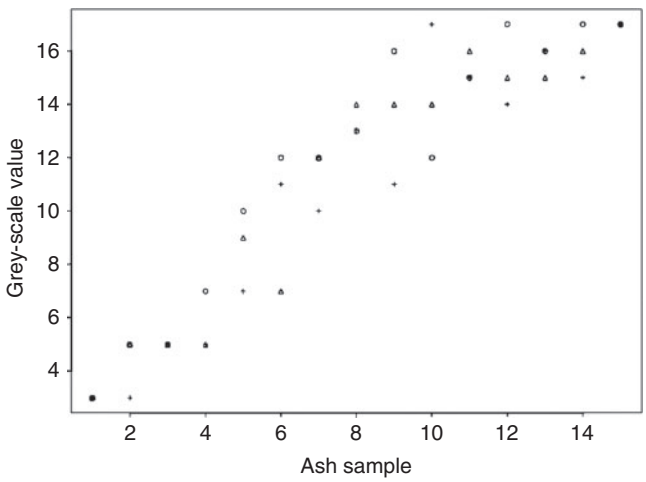

Fig. 3. Grey-scale values assessed by three individuals for each of 15 combustion residue samples. For visual convenience, the results for each sample are plotted in increasing order of mean grey-scale value as judged by the three individuals. The grey scale has 20 shades of grey labelled from 0 (white) to 19 (black) (see Fig. 1).

Results

Fig. 3 shows a plot of the grey-scale values assessed by the three individuals for each of the 15 combustion residue samples. For visual convenience, the results for each sample are plotted in increasing order of mean grey-scale value as judged by the three individuals. A range of grey scales from 3 to 17 was recorded, reflecting in part our difficulties in finding completely black char and completely white ash samples. The scatter in the *y*-axis is indicative of the degree of disagreement between the three individuals in assessing combustion residue colour-lightness, with minimum, median and maximum disagreements of 0, 2 and 5 grey shades respectively. The minimum disagreement was for the whitest and blackest samples; everyone scored them with grey scales of 3 and 17 respectively. The maximum disagreement occurred at intermediate grey-scale values. There was no clear systematic bias in any individual's assessment over the 15 samples. The median disagreement of two grey shades corresponds to 10% of the full 20 grey-shade range and is indicative of the likely precision of the measurement methodology for the data described in this paper.

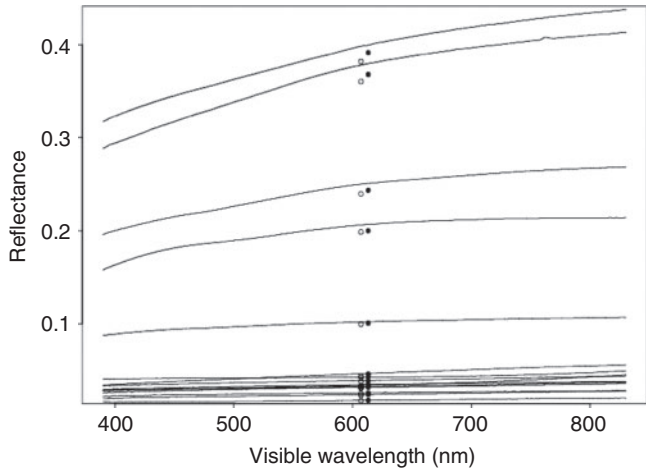

Fig. 4. The visible wavelength spectra measured by the spectroradiometer for the 15 combustion residue samples. The black filled circles show the mean visible reflectance ($\bar{\rho}$) and the unfilled circles show the mean weighted visible reflectance taking into account the spectral response of a typical human eye ($\bar{\rho}_{eye}$); they are plotted near the centre of the 390 to 830 nm range for illustrative purposes only.

Fig. 4 shows the 15 combustion residue visible wavelength spectra. The spectra are similar to certain bare soil spectra, with no blue and red wavelength absorption features found when photosynthetically active vegetation is present, and with reflectance increasing with wavelength. Five of the spectra have much higher reflectance than the other 10 spectra, and these correspond to the whiter ash samples. The spectral signatures are similar to those published by other researchers (Trigg and Flasse 2000; Pereira 2003; Roy and Landmann 2005; Smith *et al.* 2005). The filled and unfilled circles show the mean visible reflectance ($\bar{\rho}$) and the mean weighted visible reflectance taking into account the spectral response of a typical human eye ($\bar{\rho}_{eye}$) respectively. For all the spectra, $\bar{\rho}_{eye} < \bar{\rho}$. This is because the spectral response of a typical human eye is skewed to lower wavelengths over the 390 to 830 nm range (maximal at 556 nm) (Fig. 2) and because the combustion residue reflectance increases with wavelength. For the darker combustion residue samples, the difference between $\bar{\rho}_{eye}$ and $\bar{\rho}$ is <0.002 and the maximum difference (0.0094) occurs with the whitest sample. These differences between $\bar{\rho}_{eye}$ and $\bar{\rho}$ are equivalent to 4.5% (darkest sample) and 7.8% (whitest sample) of the reflectance variation over the measured visible wavelength range.

Fig. 5 shows the grey-scale values plotted against the mean weighted visible reflectance taking into account the spectral response of a typical human eye ($\bar{\rho}_{eye}$) for the 15 combustion residue samples. Fig. 5 (top) shows the three sets of grey-scale values plotted against each of the 15 $\bar{\rho}_{eye}$ values and Fig. 5 (bottom) shows the mean of the three grey-scale values plotted

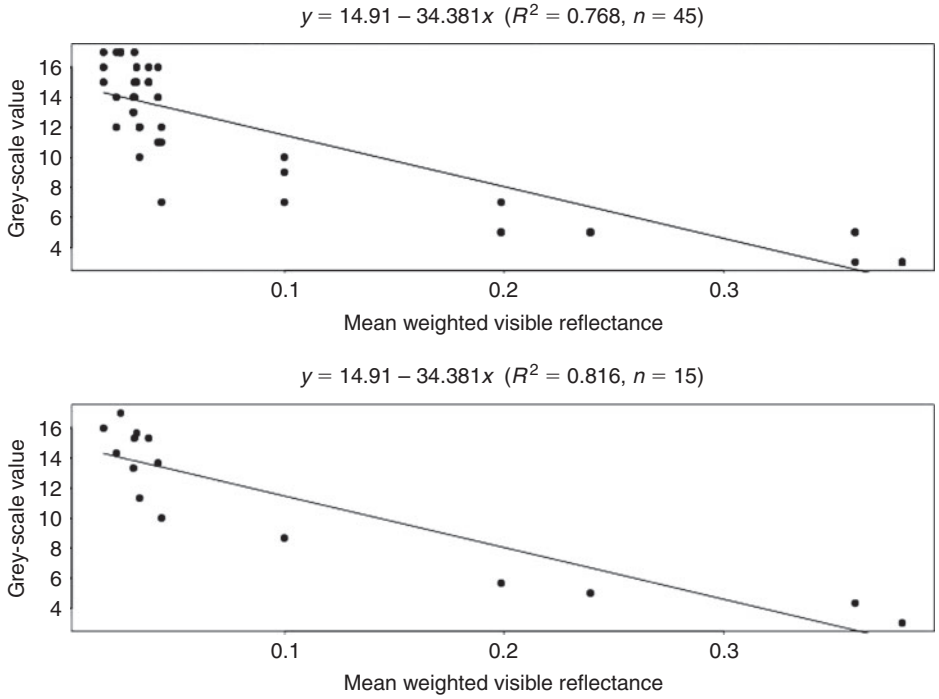

Fig. 5. Grey-scale values plotted against the mean weighted visible reflectance taking into account the spectral response of a typical human eye ($\bar{\rho}_{eye}$) for the 15 combustion residue samples. Top: the three sets of grey-scale values (Fig. 3) plotted against $\bar{\rho}_{eye}$. Bottom: the mean of the three grey-scale values plotted against $\bar{\rho}_{eye}$. There is a statistically significant relationship between the plotted data (top: $R^2 = 0.768$, $P < 10^{-14}$; bottom: $R^2 = 0.816$, $P < 10^{-5}$).

against each of the 15 $\bar{\rho}_{eye}$ values. Simple linear regression fits of these data (solid lines) and the coefficient of determination (R^2) (used to indicate goodness-of-fit) are illustrated. The regression computed using the mean grey-scale value for each combustion residue sample, rather than the three grey-scale values, has a very similar fit but inflated R^2 value (which is expected from statistical theory). In both plots, there is a statistically significant relationship between the grey-scale values and $\bar{\rho}_{eye}$ (top: $R^2 = 0.768$, $n = 45$, $P < 10^{-14}$; bottom: $R^2 = 0.816$, $n = 15$, $P < 10^{-5}$).

Humans sense brightness approximately logarithmically over a broad range of visible wavelengths (Sharpe *et al.* 2005). Taking the natural logarithm of the data in each axis of Fig. 5 provides a more linear relationship between the data. The natural logarithm of the three sets of grey-scale values plotted against the natural logarithm of the 15 $\bar{\rho}_{eye}$ values has an $R^2 = 0.891$ ($n = 45$, $P = \sim 0$) and the natural logarithm of the mean of the three grey-scale values plotted against the natural logarithm of the 15 $\bar{\rho}_{eye}$ values has an $R^2 = 0.936$ ($n = 15$, $P < 10^{-10}$).

Very similar results were found using the mean visible wavelength ($\bar{\rho}$) rather than the mean weighted visible reflectance taking into account the spectral response of a typical human eye ($\bar{\rho}_{eye}$). The results for the three sets of grey-scale values plotted against each of the 15 $\bar{\rho}$ values had only slightly smaller R^2 values (differences in the third decimal place) and slightly different slope regression coefficients (0.8 and 2% for the log-transformed and untransformed data respectively) compared with the $\bar{\rho}_{eye}$ results. The results for the mean of the three grey-scale values plotted against each of the 15 $\bar{\rho}$ values were the same as the results using $\bar{\rho}_{eye}$.

Conclusion

This paper described an experiment to assess if the colour-lightness of char and ash combustion residues could be estimated visually by comparison with a grey scale conventionally used to calibrate photographic equipment. Fifteen combustion residue samples with colour-lightness ranging from black char to white mineral ash were collected in the Northern Territory, Australia, during the dry season. The combustion residue colour-lightness was evaluated visually under controlled conditions by three individuals. The minimum, median and maximum disagreements among the three individual's independent grey-scale assessments were 0, 2 and 5 shades of grey respectively. The maximum disagreement occurred for intermediate grey shades and highlights the challenges prevalent when visually assessing post-fire effects on vegetation and soils (Lentile *et al.* 2006). The median disagreement corresponds to 10% of the grey shade range and is indicative of the likely precision of the grey-scale measurement methodology for the data described in the present study. We suggest that this 10% precision is acceptable for field measurement of combustion residue colour-lightness given the relatively quick and inexpensive nature of the grey-scale measurement approach.

Ground-based measurement of char and ash reflectance has been undertaken with portable field spectroradiometers, but spectroradiometers are expensive and delicate, and they

cannot be used to quickly measure reflectance over large areas. In this study, a calibrated field spectroradiometer was used to measure the visible wavelength (390–830 nm) reflectance spectra of each combustion residue sample. The mean visible reflectance was derived as the arithmetic mean reflectance from 390 to 830 nm, and also as a weighted mean taking into account the spectral response of a typical human eye under natural daylight conditions. The grey-scale scores for the 15 combustion residue samples were compared with the 15 mean visible wavelength combustion residue reflectance values. In all cases, there was a significant linear relationship between the grey-scale scores and the mean visible reflectance ($R^2 = 0.816$ with a linear fit, $R^2 = 0.936$ with a logarithmic transformed fit). There was no significant difference between the results derived using the arithmetic mean and the weighted mean visible reflectance values, indicating that the simpler arithmetic mean can be used.

The results of this study indicate that visual assessment using a grey scale, if repeated independently by at least three operators, provides a reliable and inexpensive way to map the colour-lightness of combustion residues. This study was performed under dry conditions in the Northern Territory, Australia. The developed grey-scale field measurement approach should not be undertaken where there are spatial variations in surface moisture, as the visible reflectance of combustion residues, like soil, is sensitive to water presence (Lobell and Asner 2002). Further research is needed to establish if the significant linear relationship between the grey-scale values and mean visible combustion residue reflectance is found under different environmental conditions, and for different fuels, fuel properties, and fire behaviours.

The colour-lightness of combustion residues is a qualitative parameter describing the post-fire condition of burned areas, and has been correlated with the completeness of combustion, fire intensity, and fire duration (Stronach and McNaughton 1989; McNaughton *et al.* 1998; Landmann 2003; Roy and Landmann 2005; Smith *et al.* 2005, 2007; Lentile *et al.* 2009). Spatially explicit mapping of combustion residue colour-lightness over a fire-affected area provides the potential for characterisation of the spatial variability of fire characteristics and effects. This methodology may provide a complementary, and perhaps less subjective and more transferable way, to field validate post-fire effects on vegetation and soil than current fire severity field assessment methods (Key 2006), especially when evaluating fire effects in wildland fires where prefire field data may not be available. Further research to verify this potential approach is needed, for example, by having several groups of individuals, each equipped with a Global Positioning System and with a grey scale, assess combustion residue colour-lightness across an extensive burn that has known fire characteristics and fire effects.

Acknowledgements

This work could not have been carried out without the support of WALFA project personnel, West Arnhem Land traditional owners, and the North Australian Indigenous Land and Sea Management Alliance (NAILSMA). This work was partly funded by NASA Earth System Science grant NNG04HZ18C and by NASA Earth Science Applications Feasibility Studies grant NNX09AO12G.

References

Analytical Spectral Devices (2002) 'FieldSpec Pro – User's Guide.' (Analytical Spectral Devices: Boulder, CO)

Byram GM (1959) Combustion of forest fuels. In 'Forest Fire: Control and Use'. (Ed. KP Davis) pp. 61–89. (McGraw Hill: New York)

Edwards A, Russell-Smith J (2009) Ecological thresholds and the status of fire-sensitive vegetation in western Arnhem Land, northern Australia: implications for management. *International Journal of Wildland Fire* **18**(2), 127–146. doi:10.1071/WF08008

Eismann K, Duggan S (2008) 'The Creative Digital Darkroom.' (O'Reilly Media: Sebastopol, CA)

Key CH (2006) Ecological and sampling constraints on defining landscape fire severity. *Fire Ecology* **2**(2), 34–59. doi:10.4996/FIREECOLOGY.0202034

Landmann T (2003) Characterizing sub-pixel Landsat ETM+ fire severity on experimental fires in the Kruger National Park, South Africa. *South African Journal of Science* **99**, 357–360.

Lentile LB, Holden Z, Smith AMS, Falkowski MJ, Hudak AT, Morgan P, Lewis SA, Gessler PE, Benson NC (2006) Remote sensing techniques to assess active fire and post-fire effects. *International Journal of Wildland Fire* **15**(3), 319–345. doi:10.1071/WF05097

Lentile LB, Smith AMS, Hudak AT, Morgan P, Bobbitt M (2009) Remote sensing for prediction of 1-year post-fire ecosystem condition. *International Journal of Wildland Fire* **18**, 594–608. doi:10.1071/WF07091

Lobell DB, Asner GP (2002) Moisture effects on soil reflectance. *Soil Science Society of America Journal* **66**, 722–727.

McNaughton SJ, Stronach NRH, Georgiadis NJ (1998) Combustion in natural fires and global emissions budgets. *Ecological Applications* **8**(2), 464–468. doi:10.1890/1051-0761(1998)008[0464:CINFAG]2.0.CO;2

Pereira JMC (2003) Remote sensing of burned areas in tropical savannas. *International Journal of Wildland Fire* **12**, 259–270. doi:10.1071/WF03028

Pereira JMC, Bernardo M, Privette JL, Caylor KK, Silva JMN, Sá ACL, Ni-Meister W (2004) A simulation analysis of the detectability of understory burns in Miombo woodlands. *Remote Sensing of Environment* **93**, 296–310. doi:10.1016/J.RSE.2004.01.009

Roy DP, Landmann T (2005) Characterizing the surface heterogeneity of fire effects using multitemporal reflective wavelength data. *International Journal of Remote Sensing* **26**, 4197–4218. doi:10.1080/01431160500112783

Roy DP, Boschetti L, Justice CO, Ju J (2008) The Collection 5 MODIS Burned Area Product – global evaluation by comparison with the MODIS Active Fire Product. *Remote Sensing of Environment* **112**, 3690–3707. doi:10.1016/J.RSE.2008.05.013

Russell-Smith J, Murphy BP, Meyer M, Cook GD, Maier S, Edwards AC, Schatz J, Brocklehurst P (2009) Improving estimates of savanna burning emissions for greenhouse accounting in northern Australia: limitations, challenges, applications. *International Journal of Wildland Fire* **18**, 1–18. doi:10.1071/WF08009

Sanches ID, Tuohy MP, Hedley MJ, Bretherton MR (2009) Large, durable and low-cost reflectance standard for field remote sensing applications. *International Journal of Remote Sensing* **30**, 2309–2319. doi:10.1080/01431160802549377

Scholes RJ, Kendall J, Justice CO (1996) The quantity of biomass burned in southern Africa. *Journal of Geophysical Research* **101**, 23 667–23 676. doi:10.1029/96JD01623

Sharpe LT, Stockman A, Jagla W, Jägle H (2005) A luminous efficiency function, V*(λ), for daylight adaptation. *Journal of Vision* **5**(3), 948–968.

Shea RW, Shea BW, Kauffman JB, Ward DE, Haskins CI, Scholes M (1996) Fuel biomass and combustion factors associated with fires in savanna ecosystems of South Africa and Zambia. *Journal of Geophysical Research* **101**, 23 551–23 568. doi:10.1029/95JD02047

Smith AMS, Hudak AT (2005) Estimating combustion of large downed woody debris from residual white ash. *International Journal of Wildland Fire* **14**, 245–248. doi:10.1071/WF05011

Smith AMS, Wooster MJ, Drake NA, Dipotso FM, Falkowski MJ, Hudak AT (2005) Testing the potential of multispectral remote sensing for retrospectively estimating fire severity in African savannahs. *Remote Sensing of Environment* **97**(1), 92–115. doi:10.1016/J.RSE.2005.04.014

Smith AMS, Lentile LB, Hudak AT, Morgan P (2007) Evaluation of linear spectral unmixing and dNBR for predicting post-fire recovery in a North American ponderosa pine forest. *International Journal of Remote Sensing* **28**(22), 5159–5166. doi:10.1080/01431160701395161

Souza CM, Roberts DA, Cochrane MA (2005) Combining spectral and spatial information to map canopy damage from selective logging and forest fires. *Remote Sensing of Environment* **98**, 329–343. doi:10.1016/J.RSE.2005.07.013

Stronach NRH, McNaughton SJ (1989) Grassland fire dynamics in the Serengeti ecosystem, and a potential method of retrospective estimating fire energy. *Journal of Applied Ecology* **26**, 1025–1033. doi:10.2307/2403709

Trigg SN, Flasse SP (2000) Characterizing the spectral–temporal response of burned savannah using *in situ* spectroradiometry and infrared thermometry. *International Journal of Remote Sensing* **21**, 3161–3168. doi:10.1080/01431160050145045

Trollope WSW, Tainton NM (1986) Effect of fire intensity on the grass and bush components of the Eastern Cape Thornveld. *African Journal of Range and Forage Science* **3**(2), 37–42.

Williams RJ, Gill AM, Moore PHR (1998) Seasonal changes in fire behaviour in a tropical savanna in northern Australia. *International Journal of Wildland Fire* **8**(4), 227–239. doi:10.1071/WF9980227

Wooster MJ, Roberts G, Perry GLW, Kaufman YJ (2005) Retrieval of biomass combustion rates and totals from fire radiative power observations: FRP derivation and calibration relationships between biomass consumption and fire radiative energy release. *Journal of Geophysical Research* **110**, D24311. doi:10.1029/2005JD006318

Yates CP, Edwards AC, Russell-Smith J (2008) Big fires and their ecological impacts in Australian savannas: size and frequency matters. *International Journal of Wildland Fire* **17**, 768–781. doi:10.1071/WF07150

Manuscript received 18 November 2009, accepted 17 April 2010